Recent Trends in the Frequency and Duration of Global Floods

Nasser Najibi[1,2,3] and Naresh Devineni[1,2,3]

[1]Department of Civil Engineering, City University of New York (City College), New York 10031, USA
[2]Center for Water Resources and Environmental Research (City Water Center), City University of New York, New York 10031, USA
[3]NOAA/Cooperative Science Center for Earth System Sciences and Remote Sensing Technologies (CREST), City University of New York, New York 10031, USA

Correspondence to: Nasser Najibi (nnajibi@ccny.cuny.edu)

Abstract. Frequency and duration of floods are analyzed using the Dartmouth Flood Observatory's (DFO) global flood database to detect the significant trends during 1985-2015 at the global and the latitudinal scales. Three classes of flood duration (i.e., short: 1-7, moderate: 8-20, and long: 21 days and above) are also considered for this analysis. The non-parametric Mann-Kendall trend analysis is used to evaluate three hypotheses (H1, H2, and H3) addressing potential monotonic trends in the frequency of flood, moments of the duration, and the frequency of specific flood duration types. Results show that long duration flood frequency has increased both at the global and the latitudinal scales. In the tropics, floods have increased four-fold since the 2000s. This increase is 2.5-fold in the north mid-latitudes. There is no monotonic trend in the frequency of short duration floods across all the global and latitudinal scales. There is a significant increasing trend in the annual median and tails of flood durations globally and in each latitudinal belt. We evaluated hypothesis H4 to identify possible large-scale and atmospheric teleconnections that can explain the trends using a Generalized Linear Model framework. This analysis provides insights for understanding the frequency and persistence in hydrologic extremes and how they relate to changes in the climate, organization of global and local dynamical systems and socioeconomic factors.

1   Introduction

Higher levels of vulnerabilities to extreme events, especially floods, are becoming a "new normal" in both developing and developed countries. There is rapidly growing population, assets, and expanding residential and commercial sectors that are susceptible to damages during these events (Mirza, 2003; Thomalla et al., 2006; Hallegatte et al., 2013; Singh and Zommers, 2014). Moreover, while flood-related fatalities have substantially decreased in recent decades mainly due to improved early warning systems and better flood control infrastructure, statistics still point out that there are people (in)directly affected by these events. For instance, Guha-Sapir et al. (2016) in their annual disaster statistical review of 2016 reported that the number of people affected by hydrologic disasters (floods or landslides) is 78.1 million, approximately 13.7% of all people affected in 2016. It is also striking to note that 60 million of these 78.1 million people were affected by one flood in China.

Other impacts of floods include various deteriorations of social services, economic disruptions, health-related issues, and consequences of population displacement (i.e., disturbances in food supply chain, under-nutrition, water/vector-borne diseases,

and being injured, displaced or left homeless) (Schultz, 2006; Milojevic et al., 2011; Lowe et al., 2013). An unusual increase in the bacillary dysentery risk in Baise (Guangxi Province, China) during the years 2004 to 2012 is a case in point (see more details in Liu et al. (2017)). The recent Thailand floods that occurred in July 2011 and December 2014 also caused severe supply chain disruptions (Ziegler et al., 2012; Haraguchi and Lall, 2015; Promchote et al., 2016).

5 Often, these impacts are magnified when the floods are due to persistent and recurrent rainfall. Such floods typically last longer (henceforth called long duration floods) and are associated with repeated rainfall events in the regions. Recently, Robertson et al. (2011), Nakamura et al. (2013), Lu et al. (2013), Ward et al. (2015), Haraguchi and Lall (2015), Najibi et al. (2017), Gao et al. (2017), Lu and Lall (2017), and Lu and Hao (2017) have attempted to quantify the causal mechanisms and impacts of such long duration floods at the regional scale. An important question in this context is whether we understand the planetary

10 nature of the trends in the frequency and duration of these long-duration floods. Understanding the global trends and quantifying their potential climate-related attributes can help improve flood forecasting systems and in better management of flood control infrastructure.

Global and near-daily observations from the Earth's surface are now available through satellite microwave sensors (active/passive) which are being employed to measure the changes of water surfaces (e.g., river discharge and watershed runoff)

15 (Brakenridge et al., 2007). Utilizing such information even with limited ground-based discharge data can allow the mapping of flood inundation extents at many locations around the world. Such satellite-based measurements have a particular advantage in understanding the impacts of floods in developing nations where there is lack of sufficient in-situ measurements (Brakenridge et al., 2007; Van Dijk et al., 2016; Brakenridge et al., 2016). In this study, we provide a global-scale analysis of the recent trends in the frequency and probability distribution of the duration of floods provided by such satellite imagery products with

20 an objective to understand the trends from the context of ocean-atmospheric interactions and socioeconomic factors.

Given the floods (especially the long duration floods) are caused by a systematic organization of the global-to-local dynamical systems of climate and atmosphere (Najibi et al., 2017), characterizing the temporal trends (regime like behavior) will help us to understand better, the frequency and persistence in the organization of these systems. We can use this understanding to explore their predictability using state space models (Abarbanel and Lall, 1996; Karamperidou et al., 2014; Perdigão and

25 Blöschl, 2015). Together, the characterization of the trends and the predictability of these extremes will enable us to improve the climate impact assessment and understand whether or not a regional persistent flood regime is likely to end or continue.

Consequently, we utilized the global active archive of flood events (with 31 years of data from 1985 to 2015) to address the following five questions:

1. How has the annual frequency of floods changed at the global scale and various latitudinal belts during the last three
30 decades?

2. How has the probability distribution of flood duration (i.e., the moments and extreme values) changed at the global scale and various latitudinal belts during the last three decades?

3. Are the changes (if any) in the flood frequency and the probability distribution of flood durations due to the changes in a specific flood class, i.e., short, moderate or long duration?

4. Can the changes (if any) in the flood frequency and the probability distribution of flood durations be related to the variability in the atmospheric teleconnections and low-frequency climate oscillations?

5. Which countries are most vulnerable to short, moderate and long duration floods?

We address each question using a formal hypothesis-testing framework. This paper is organized as follows: Section 2 provides the detailed information about the global flood database, design hypotheses, and employed methodology in this study. Section 3 presents the results of the hypothesis tests. In Section 4, we attribute the observed trends to potential causes using a Generalized Linear Modeling (GLM) framework and other comparable studies. Finally, we present the concluding remarks and highlights in Section 5.

2   Data, Methodology, and Hypotheses

2.1   Global active archive of flood events: Dartmouth Flood Observatory (DFO)

A comprehensive record of flood events is available from the Dartmouth Flood Observatory (DFO) founded in 1993 at the Dartmouth College, NH, United States. In 2010, the observatory moved to the Community Surface Dynamics Modeling System (CSDMS) (http://csdms.colorado.edu/) as a division of Institute of Arctic and Alpine Research (INSTAAR) at the University of Colorado, Boulder, United States (Brakenridge, 2010). Information in this archive is based on instrumental measurements and remote sensing sensors. These events are validated based on officially reported flood details by governmental and news agencies (Brakenridge et al., 2016). DFO mostly takes advantage of orbital remote sensing sensors to identify, measure and monitor global flood events by gathering globally consistent information on surface water changes, in particular since 1999. Floods are detected using MODIS (Moderate-resolution Imaging Spectroradiometer) sensors (approximately 250-m footprint pixel), and river discharges are measures using satellite microwave data such as AMSR-E (Advanced Microwave Scanning Radiometer for EOS -Earth Observation System- from Global Change Observation Mission-Water (GCOM-W)). The discharge values and runoff coefficients are then calculated from the Water Balance Model (WBM) embedded with the specific soil type, surface gradient, soil permeability, and land use/land cover (LULC) characteristics. These remote sensing and model outputs are employed conjunctively to map the potential flood inundation extents frequently. Then, a number is assigned to the flood if a) it is unusually "large" compared to the typical annual high water and previously mapped water-land extents, and/or b) if there are significant damages caused to the structures, extensive land inundation, and fatalities (Brakenridge et al., 2016).

It is important to note that the quality of data has improved in the recent times. The improvements in the level of media reporting and information quality have improved the reliability of the data. At the same time, the likely improvements in the accuracy of in-situ measurements, advances in satellite and ground-based sensors, data storage, and transfer facilities also contributed to the data quality. Moreover, Brakenridge et al. (2003), Brakenridge et al. (2005), and Brakenridge et al. (2012) have discussed that the frequent temporal sampling of satellite-based observations and ground sources (media reporting) determines the accuracy level amongst the (non-)flood event candidates. The dataset covers flood events at the global scale from January 1, 1985, to present. Any recent flood event is added immediately to the data archive. In this study, we considered 31

years of global flood events from January 1, 1985, to December 31, 2015. This comprehensive dataset includes information on the location of a flood event (longitude, latitude, and the name of the country), flood beginning and end date, damages due to flood, and its duration. The DFO is the only global dataset of observed flood events. Much of the prior studies either focused on rainfall-based datasets or model-based river flow data. In this regard, the present study adds a new dimension to the flood

5   literature, especially the understanding of the long-duration floods on a global scale.

2.2   Aggregating floods on the basis of the latitudinal belts

The flood events are spatially aggregated to five climate zones - tropics (23.5 ºS to 23.5 ºN), northern hemisphere subtropics (23.5 ºN-35 ºN) and mid-latitudes (35 ºN-55 ºN), and southern hemisphere subtropic (23.5 ºS-35 ºS) and mid-latitudes (35 ºS-55 ºS) (*Environmental Literacy Council,* ELC (2015)). We chose these spatial aggregations along the latitudinal belts to

10   be consistent with the global circulation dynamics, zonally symmetric thermal forcing (Walker and Schneider, 2005; Zhai and Boos, 2015), temperature variabilities and precipitation patterns (Gabler et al., 2008). Besides, such specifications will result in achieving higher coherency in satellite-based data acquisition in particular for the passive sensors, because of varying solar reflectivity and ascending/descending satellite orbits along different latitudes (Thenkabail, 2015). Fig. 1 represents the schematic of the five climate zones. We also show four countries (USA, China, India, and Thailand) that have experienced high

15   rates of long duration floods from 1985 to 2015.

FIGURE 1

Next, for each latitudinal belt, the total number of floods per year (calendar year from January 1 to December 31), the duration of these floods and their location (name of country) are processed. This procedure is formulated as follows:

$$F_C^{t;r} = \text{Total number of flood event(s) in latitudinal belt } r \text{ and year } t \tag{1}$$

20   $$\boldsymbol{F_D^{t;r}} = \text{Duration(s) of flood event(s) in latitudinal belt } r \text{ and year } t \text{ [day(s)]} \tag{2}$$

$$\boldsymbol{F_L^{t;r}} = \text{Location(s) of flood event(s) in latitudinal belt } r \text{ and year } t \text{ [name of country(ies)]} \tag{3}$$

where F_C indicates the flood counts (frequency), and $\mathbf{F_D}$ and $\mathbf{F_L}$ denote the vectors of flood duration and flood location for each of these flood events respectively. The superscripts r and t denote the latitudinal belt (r= {global, tropics, mid-latitudes (N and S), subtropics (N and S)}), and year (t= {1985, 1986,..., 2015}).

25   In addition, the number of floods in each latitudinal belt are also categorized in terms of their *duration*. We denote the event as a short duration flood $F_{C_\mathrm{S}}^{t;r}$ if the duration is between 1 and 7 days; moderate duration flood $F_{C_\mathrm{M}}^{t;r}$ if the duration is between 8 and 21 days; and as long duration flood $F_{C_\mathrm{L}}^{t;r}$ if the duration is greater than or equal to 21 days. These categories are also

consistent with the DFO's flood classification (Brakenridge, 2010). The subscripts S, M and L stand for *Short*, *Moderate* and *Long* duration flood events respectively.

2.3 Atmospheric teleconnections and climate indices

We used large-scale ocean-atmospheric teleconnections to investigate the extent to which the trends in the floods can be related to natural variability (Enfield et al., 2001; Ward et al., 2016) in the climate-atmospheric system. Since the climate system has as quasi-periodic nature that often manifests as wet and dry regimes, it is important to understand whether the trends, if observed, can be attributed to these natural oscillations. Hence, we used El Nino-Southern Oscillation (ENSO), Pacific Decadal Oscillation (PDO), North Atlantic Oscillation (NAO), and Atlantic Multidecadal Oscillation (AMO) as proxies for interannual, decadal and multidecadal climate variability.

We obtained 31 years (1985 - 2015) of ENSO data (aggregated based on the monthly anomalies of Niño 3.4) from the HadISST1 dataset (Rayner et al., 2003). Monthly AMO and PDO anomalies obtained from the NOAA/Earth System Research Laboratory at http://www.esrl.noaa.gov/psd/data/climateindices/list (Zhang et al., 1997), and then averaged to yearly time series from 1985 to 2015. Similarly, the monthly NAO indices obtained from the NOAA/National Weather Service, Climate Prediction Center at http://www.cpc.ncep.noaa.gov/products/monitoring_and_data/ (Barnston and Livezey, 1987; Hurrell and Van Loon, 1997) are averaged to yearly time series.

2.4 Calculating resistant metrics from the distribution of flood duration

In addition to the frequency of floods ($F_C^{t,r}$), we calculate a set of "resistant measures" to evaluate the existence of any significant monotonic time trend in the probability distribution of flood duration. Four moment indicators are selected because of their scale-invariant characteristics suitable for such asymmetric distributions. These metrics include the median, median absolute deviation (MAD), resistant skewness, and the 90th percentile of the distribution of flood durations in each year. Each of these metrics is computed as a time series of 31 years (1985 - 2015) for each of the six spatial scales (i.e., global, tropics, mid-latitudes (N), mid-latitudes (S), subtropics (N), subtropics (S)). It is straightforward to calculate the median and 90th percentile from the distribution of flood duration each year. We explain the formulation and the properties of the other two metrics here:

2.4.1 Median Absolute Deviation (MAD) of flood durations

We calculate the Median Absolute Deviation (MAD) of flood duration as an indicator of the deviation from the central tendency. The MAD is a robust measure to quantify the within-year variation of flood duration. It is a good measure of scale for distributions with heavier tails (Sachs, 2012). It is also resistant to the influence of outliers (Hampel, 1974). Contrary to the standard deviation (SD) -which is affected by non-normality of probability distribution and extremely high/low values- the presence of outliers does not change the MAD value (Leys et al., 2013). However, the interpretation of MAD is similar to SD;

as it measures the deviation from the average flood duration. MAD is computed as follows:

$$\boldsymbol{F_{D_{MAD}}^{t,r}} = median\left(\|\boldsymbol{F_D}^{t,r} - F_{D_{Median}}^{t,r}\|\right) \tag{4}$$

where t, r, and $\boldsymbol{F_D}^{t,r}$ are the same variables defined in Equation 2 and $F_{D_{Median}}^{t,r}$ is referred to the median of distribution of flood duration.

5 2.4.2 Resistant skewness of flood durations

The presence of outliers amongst the variables will generate a large and possibly misleading measure of skewness (Helsel and Hirsch, 1992). Instead, the resistant skewness is a more robust measure for capturing the asymmetrical/symmetrical properties in the data. It is estimated using the following equation:

$$F_{D_{rSkewness}}^{t,r} = \frac{\left(F_{D_{0.75}}^{t,r} - F_{D_{Median}}^{t,r}\right) - \left(F_{D_{Median}}^{t,r} - F_{D_{0.25}}^{t,r}\right)}{\left(F_{D_{0.75}}^{t,r} - F_{D_{0.25}}^{t,r}\right)} \tag{5}$$

10 where $F_{D_{rSkewness}}^{t,r}$ is the resistant skewness of flood duration, r and t are the same variables previously given in Equation 2, $F_{D_{0.25}}^{t,r}$ and $F_{D_{0.75}}^{t,r}$ refer to the 25th and 75th percentiles of flood durations for each year for the specified latitudinal belt.

Note that the sample sizes (number of floods) may be different for different years. For instance, the total number of floods in 1985 at the global scale is 69. We compute the median, MAD, skewness and the 90th percentile of the duration for these 69 events. Similarly, the total number of floods in 2015 at the global scale is 101, and we compute the median, MAD, skewness 15 and the 90th percentile for these 101 events. After obtaining the time series of these metrics, we then investigate for monotonic time trends.

2.5 Hypotheses

Most of the global precipitation studies indicate that there is a recent increase in both the annual precipitation and extreme rainfall intensities (Solomon, 2007; Zhou et al., 2013). Consequently, our goal here is to investigate whether we see a significant 20 trend in the frequency and duration of floods during the last three decades.

The main hypotheses (**H1**, **H2**, **H3**, and **H4**) and the evaluation procedure are presented in Table 1. We begin our investigation with **H1**, the hypothesis that there is no monotonic trend in the annual frequency of the flood events. We test this hypothesis using the Mann-Kendall (MK) trend test (Mann, 1945). With **H2**, we are exploring whether there is a change in the probability distribution of the flood duration over time. We test this hypothesis by applying the MK trend test on the three resistance 25 moments (median, median absolute deviation, and skewness) and the 90th percentile (extreme flood duration) of the annual distribution of flood duration. **H3** is intended to investigate the changes in the patterns of flood frequencies for each category: short, moderate and long duration floods. Lastly, in **H4**, we investigate the potential large-scale atmospheric teleconnection factors that the observed trend(s) in H1 and H2 can be attributed to, using a Generalized Linear Model (GLM) framework.

TABLE 1

2.6 The Generalized Linear Model (GLM) Framework

Our hypothesis (i.e., **H4**) is that the detected time trend is due to cyclical climate influences (i.e., oscillatory behavior) associated with the large-scale ocean-atmospheric interactions. Hence, for all the cases where the null hypothesis of *no trend* is rejected, we attempted to understand whether the trend relates to large-scale climate oscillations. For this purpose, we employed a Generalized Linear Model (GLM) framework on the time-series of the above-developed metrics with ENSO, AMO, PDO, and NAO as predictors (i.e., covariates). GLMs are the mathematical extension of classical linear regression models to include a broad class of model assumptions such as linear, Poisson, exponential, log-linear and so on with specified link functions (McCullagh, 1984; Yang et al., 2005; Chandler and Wheater, 2002). For all the spatial scales where we see a statistically significant trend, a Generalized Linear Model is fit to the time series (1985 - 2015) of F_C, $F_{D_{Median}}$, and $F_{D_{90}}$ with climate covariates as:

$$F_C = a + b_1 ENSO + b_2 AMO + b_3 PDO + b_4 NAO \tag{6}$$

$$F_{D_{Median}} = a + b_1 ENSO + b_2 AMO + b_3 PDO + b_4 NAO \tag{7}$$

$$F_{D_{90}} = a + b_1 ENSO + b_2 AMO + b_3 PDO + b_4 NAO \tag{8}$$

where a, b_1, b_2, b_3, and b_4 are the GLM's coefficients (parameters). We then select the best model using the forward and backward stepwise regression and obtain the residuals of the best model in each case. The residuals represent the values for F_C, $F_{D_{Median}}$, and $F_{D_{90}}$ after adjusting for exogenous variables. In other words, they reveal the variability beyond what could be attributed to exogenous climate factors. The analysis of the time trends in the residuals will help to discern any unexplained trend after accounting for background variability due to climatic modulation. The models are fit using the stepwiseglm toolbox in Matlab 2017b (McCullagh, 1984) that uses the forward and backward regression algorithm. We used the Deviance Information Criterion for the best model selection among a finite set of models. Results from the models are presented in Section 4 where we discuss the associations.

3 Results

3.1 Addressing H1: Trends in the annual frequency of flood events

Mann-Kendall (MK) test (Equation A1-A3) is applied to each time series of F_C (i.e., global, tropics, mid-latitudes (N), mid-latitudes (S), subtropics (N) and subtropics (S)) for the detection of monotonic trends. The MK test uses ranks of the data and assumes no underlying probability distribution (Helsel and Hirsch, 1992). The test statistic is based on the pairwise comparison between the values and is independent of the distribution of the original series. The magnitude of the slope of the trend is

estimated using the method of Sen, the median of the pairwise slopes between the elements of the series (Sen, 1968). Ties in the data are adjusted using an assumption that the number of ties is equal to an even number of positive and negative differences (Burkey, 2006).

Statistical significance is evaluated at a 5% significance level, the probability of incorrectly rejecting the null hypothesis. Figure 2 presents the time series of F_C for the global scale and the five latitudinal belts. A solid LOESS (LOcal regrESSion) curve is shown if the trend is significant. Alternately, a dashed LOESS curve is shown for the time series that do not exhibit a statistically significant trend. The detailed statistics derived from the trend analysis are given in Table 2.

FIGURE 2

TABLE 2

A total of 4311 flood events occurred during last three decades worldwide. The results of MK test on the annual frequency of global floods indicate that there is a statistically significant monotonic trend with τ (Kendall correlation coefficient between F_C and time) and β (robust Sen Slope) values of 0.26 and 2.12, respectively. A total of 2020 events (out of the 4311 floods) occurred across the tropics. The hypothesis that there is no trend in the frequency of floods in the tropics is also rejected. This is also the case for both subtropics (S) and mid-latitudes (S). However, while we see an uptrend in the number of floods in mid-latitude (S) post-2000, we urge caution in interpreting this trend as zeros dominate the time series. Finally, for both subtropics (N) and mid-latitudes (N), the hypothesis that there is no trend in the annual frequency of floods cannot be rejected.

- **H1**: There is a statistically significant increase in the frequency of floods at the global scale, and over the tropics, subtropics (S), and mid-latitudes (S). The temporal pattern of the data for global floods resembles that of the tropics and the sub-tropics (S).

3.2 Addressing H2: Trends in the distribution of flood duration

The MK trend tests are performed on the time series of the median, median absolute deviation (MAD), resistant skewness, and the 90th percentile of the flood duration. The following four subsections elaborate the results for each metric.

3.2.1 Trends in the median of flood durations

From Figure 3, we can see that there is a statistically significant monotonic trend in the median of the flood duration at the global scale and all sub-spatial scales. We see that the median of the flood duration at the global scale has increased steadily from four days in the year 1985 to ten days in the year 2015. Similar shifts can be observed in the tropics and the subtropics. In Table 3, we present the statistics of the tests. As in the case of the frequency of floods, we urge caution in interpreting the trends seen in mid-latitude (S).

FIGURE 3

TABLE 3

3.2.2 Trends in the Median Absolute Deviation (MAD) of flood durations

The MK trend test is performed on the MAD of flood duration (Equation 4) at the different global and latitudinal scales and presented in Figure 4 and Table 4.

FIGURE 4

TABLE 4

The output statistics show that there is a significant increasing trend in MAD at the global scale, and in the tropics and subtropics (N). It is interesting to note that the MAD has essentially remained constant, around 2 - 3 day from 1985 to 2000 and has increased since to around five days in 2015. There is no significant change in the variability in the mid-latitudes (N and S) and subtropics (S).

3.2.3 Trends in the resistant skewness of flood duration

The resistant skewness of flood duration is calculated for each time series using Equation 5 and presented in Figure 5. As before, MK trend test is applied to these time series. A statistically significant trend in the skewness is observed at the global scale, tropics, and the subtropics (S) latitudes. Similar to Tables 2, 3 and 4, in Table 5, we present the test statistics. We observe that the yearly asymmetrical/symmetrical behavior of the distribution of flood durations has considerably changed during the recent three decades (from 5 to 8 approximately) with a more significant tendency towards high skewness. Conversely, there is no significant trend in the skewness of flood duration in subtropics (N) and mid-latitudes (N).

FIGURE 5

TABLE 5

3.2.4 Trends in the 90th percentile of flood durations

Finally, we test for monotonic trend in the extreme values (expressed here as 90th percentile) of flood duration. This measure serves as a surrogate for extremely long duration flood events each year. By definition, the 90th percentile of the flood duration $(F_{D_{90}}^{t,r})$ is the value which is exceeded by only ten percent of the events in that year (year t) in the latitudinal belt r. Consequently, a value as large as this indicates the long-duration extent of the flood. Figure 6 and Table 6 present the summary of MK analysis on the 90th percentile of flood duration.

FIGURE 6

TABLE 6

The duration of floods has substantially changed over the recent three decades at the global scale, tropics, mid-latitudes (N and S) and subtropics (S), as presented in Table 6. The null hypothesis that there is no monotonic trend in the tails is rejected in all

regions, except the sub-tropics (N). Furthermore, we find that the extreme values of the duration flood events are more than 30 days in the 2000s, whereas they were less than 20 days in the 1980s and 1990s. Unlike the case of MAD where we found an abrupt shift post-2000, the 90th percentile of the flood duration exhibit a small linear trend over the 30 years.

The highlights of trend analyses presented in Figures 3 to 6 and Tables 3 to 6 are outlined below:

- **H2**: The median of flood duration has increased at the global scale and all sub-spatial scales. There is also an increasing monotonic trend in the MAD of flood duration across the global, tropics, and subtropics (N) spatial scales. We also see an increase in the resistant skewness of flood duration around the globe, tropics, subtropics (S) and the mid-latitudes (S). For the extreme flood durations (i.e., 90th percentile), we see an increasing trend in all spatial scales except the subtropics (N) over past three decades. Due to the presence of a significant number of zeros in the statistics of the floods, we urge caution in interpreting the trends seen in the mid-latitudes (S).

3.3   Addressing H3: Trends in the frequency of short, moderate and long duration floods

Given that we find statistically significant trends in the tails of the distribution (90th percentile of the duration of floods), we were interested in exploring whether there would be a trend in the frequency of the long duration floods as well. To investigate this, we performed the MK test on the frequency of long duration floods (F_{C_L}) for tropics, subtropics, and mid-latitudes. We also performed these tests on short duration flood frequency (F_{C_S}) and moderate duration flood frequency (F_{C_M}). We present these results in Table 7.

As it can be seen from Table 7, there is no monotonic trend in the frequency of short duration floods occurring across all the spatial scales, indicating that the number of short duration floods has not changed significantly over the last three decades worldwide. However, this phenomenon is not true for moderate and long duration floods. In fact, the frequency of both moderate and long duration floods has increased in the tropics. These findings are consistent with the results from H2. There is also an increasing trend in moderate duration floods in the subtropics (S) and long duration floods in the mid-latitudes (N).

TABLE 7

For the long duration flood events in tropics, the total number of events has increased from 60 before 2000 to 249 after 2000. Similarly, the total number of events in the mid-latitudes has increased from 27 to 70 post-2000. In other words, long duration floods occurred during recent 15 years are four times more than before the year 2000. The increase across the mid-latitudes (N) is around 2.5 times pre and post-2000.

In summary:

- **H3**: Frequency of moderate and long duration flood classes has changed recently, but remain unchanged for the short duration floods in all the latitudinal belts. The annual frequencies of moderate and long duration flood events have increased across the tropics and mid-latitudes (N) (on the scale of 4 and 2.5 events per year, respectively) over last three decades.

3.4 Country scale vulnerability analysis to short, moderate and long duration flood events

There were 4311 flood events that occurred from 1985 to 2015 around the world. According to Table 2 and Table 7, globally, the total number of short, moderate and long duration flood events were 2508 ($\approx$59%), 1151 ($\approx$27%), and 560 ($\approx$13%), respectively. In addition to the aggregate analyses at the latitudinal level, we also explored the country scale vulnerability to short, moderate, and long duration floods. We interpret vulnerability as the expected value of the damage due to floods (the severity of the consequence of the floods) (Holling, 1978; Hashimoto et al., 1982). The consequences of floods should be paid attention to as this plays a big role in designing appropriate flood-proofing infrastructure and developing early warning systems and flood insurance payout structures. The relation between the duration of the floods and the damages, and how they vary across different countries is also of interest here.

For this purpose, we first excluded countries which had less than 31 flood events to ensure that we investigate only those counties that have experienced at least one flood per year on the average. This screening resulted in 28 countries with a minimum of 31 flood events during the last three decades. These 28 flood-prone countries are sorted as follows: USA (388 events), China (344 events), India (226 events), Indonesia (190 events), Philippines (181 events), Australia (121 events), Vietnam (107 events), Brazil (96 events), Bangladesh (88 events), Mexico (80 events), Iran (77 events), Afghanistan (74 events), Russia (69 events), Thailand (66 events), Pakistan (66 events), Nigeria (57 events), Malaysia (54 events), Kenya (49 events), Canada (48 events), Colombia (44 events), Peru (43 events), Turkey (41 events), Nepal (40 events), France (40 events), Romania (38 events), Ethiopia (35 events), Somalia (34 events), and New Zealand (31 events).

Then, the fraction of flood frequencies for each country and duration class -short, moderate and long- is calculated. Figure 7 (a) presents these fractions for the 28 countries using the ternary plot. For 23 of these countries, we have the data on the damages due to the floods. We computed the expected value of the damages for each country and plotted the fractional damage due to short, moderate and long duration floods as the second ternary plot in Figure 7(b). The color bars indicate the total number of events (Figure 7a) and the total flood damage (Figure 7b). In each plot, the location of the country shows the relative fraction of short, moderate and long duration flood frequency and damage. For example, in Figure 7(a), the USA is identified as the red circle in the top corner with > 60% floods being short duration, between 30 and 40% of the floods being moderate and only 10% of them being long duration floods. However, in terms of the vulnerability to floods (Figure 7b), USA is located in the bottom right corner of the triangle, indicating that most of the vulnerability is due to low probability long duration floods. Similar observations can be made for Vietnam, Mexico, Indonesia, Australia, and Malaysia, to name a few. These countries have a very low probability of long-duration floods, but the consequence of these floods is the most important in terms of the vulnerability. It is also noteworthy to emphasize that for most of the countries, the overall damage is dominated by the damage due to moderate and long duration floods. This can be seen from the fact that much of the countries are found in the bottom left and right corners of the ternary plot.

FIGURE 7

To further understand the relation between flood duration and flood damage, we fit nonlinear models of the form $damage = \alpha * duration^{\beta}$ (in the log-space) for four selected countries; USA, Thailand, India and China. The results of the log-linear

models for these four countries are shown in Figure 8(a). These countries are selected because they have the highest number of long duration floods among all countries (Figure 8b). Parameter β is the scaling exponent of the damages to the flood duration. Note that the scaling exponent is similar for USA (0.89) and China (1.03) while India (0.23) and Thailand (0.56) have much smaller exponents. In total, 226 flood events occurred across India in which around 43%, 32%, and 25% of them were short, moderate and long duration events respectively. In the United States, short, moderate and long duration flood events account for 66%, 26%, and 8% of 388 flood events that occurred in last three decades. However, the fraction of long duration flood events is much higher for Thailand (30% of total flood events). In China, around half of the flood events were related to the moderate or long duration flood classes (34% and 16% respectively). This opens up new questions about whether there are consistent relations like this across the globe and how different these scaling exponents would be. We do not pursue them as part of this investigation, however, in the spirit of examining flood duration and damages, in Figure 8(b) and (c), we present the data on flood duration, and flood damage ranked for various other countries.

According to the DFO flood data from 1985 to 2015, the ranking results show that the frequency of short duration floods for the USA, China, India, and the Philippines is respectively 255, 173, 133, and 122. For moderate duration floods, the countries of China, USA, India, and the Philippines have experienced 118, 101, 74, and 52 flood events, respectively. The long duration floods were seen mostly in India (55 events), China (53 events), USA (32 events), and Thailand (20 events) from 1985 to the end of 2015. It should be noted that here we only presented the top 21 countries in each category.

FIGURE 8

4   Discussion

The trends in the frequency and the distribution of the floods (prominent in long-duration floods) may be related to several causes ranging from measurement uncertainty in the DFO flood data, climate and atmospheric teleconnections, and socioeconomic contributions such as the increased exposure to the flood events. We attempt to explain these possibilities in the following two sections:

4.1   What are the uncertainties in DFO flood archive data, and/or have the exposure to the flood events changed?

The flood archive data provided by DFO are being collected from different methods of observation and validation since 1985 (see the summary of the methods in Brakenridge et al. (2005)). Besides, there are more flood warning systems and facilities, transmitting instruments, reporting networks, and communications nowadays at different levels of social and governmental divisions that DFO is using to provide more comprehensive flood information. They have improved their flood detection methods by including the MODIS products since 1999. MODIS products contain surface inundation information based on vertically and horizontally polarized backscatters acquired remotely from the radiance changes between water, land and vegetation-covered surfaces (Brakenridge et al., 2007). We acknowledge that there could be some uncertainties as a result of this since surface may also be interpreted as water in the presence of clouds, cloud shadows, and mountainous terrain (Brakenridge et al., 1998).

While understanding such uncertainties is essential, especially while interpreting trends in limited data, it is also documented in the literature that there has been an increased exposure to floods in the recent times. The number of people, residential, industrial properties, and assets exposed to the flood events has drastically increased (Bouwer, 2011; Jongman et al., 2012; Kundzewicz et al., 2014). The type of vulnerability to the flood risk is mostly connected to the development of the country and its land-use and environmental management (Peduzzi et al., 2009). Recent studies by Di Baldassarre et al. (2010) and Vogel et al. (2011) in Africa and the United States respectively, showed that there had been a considerable change in the flood frequency and magnitude in regions which have undergone intense urbanization.

While exposure of people to floods is the main concern in developing countries, exposure of assets and properties to floods is the vital concern for the developed countries (Jongman et al., 2012). Recently, many residential and industrial infrastructure has moved to the flat and cheap lands of floodplains (Peduzzi et al., 2011). The nature of geomorphological features of land has been modified to embrace these new developments. Hirabayashi et al. (2013) and Stevens et al. (2016) have recently indicated that the increase in the reporting of floods can be linked to the rise in the land use development in the floodplains.

4.2 Can the trends be related to natural variability in the climate and atmospheric systems?

The frequency of heavy precipitation events has increased at the global scale (Groisman et al., 2005; Zhou et al., 2013; Liu and Zipser, 2015). Using daily precipitation observations from the Global Historical Climatology Network (GHCN) dataset, Alexander et al. (2006) showed that the distributions of precipitation indices in 1979–2003 period are significantly different from the 1901–1950 period with a tendency towards wetter conditions. Solomon (2007), in the fourth assessment report of the Intergovernmental Panel on Climate Change (IPCC), discussed that the annual precipitation intensity has increased over high-latitudes during the periods 1901 to 2005, except the southwest of the United States, northwestern Mexico, and the Baja Peninsula. This IPCC report also highlights the increasing contribution of extreme rainfall events to the total precipitation across Europe and the United States which mostly happened during the last three decades of the 20th century. Westra et al. (2013) tested 8326 land-based rainfall stations (with at least 30 years of record from 1900 to 2009) and found that the annual maximum daily precipitation has significantly increased for more than two-thirds of these stations at the global scale.

Theoretical studies also discussed that mean global precipitation intensity increased by 1–3% (conditional on available energy budgets) in proportion to the 1°C increasing rate of surface air temperature. Trenberth (1999), Trenberth et al. (2003), Trenberth (2011), Schiermeier (2011), and Glur et al. (2013) among others have also argued that an increase in air temperature will increase the atmospheric water-holding capacity (Clausius-Clapeyron relationship) leading to more intense and frequent precipitation events. Hence, fluctuating precipitation regimes would interrupt the current balances of components within the hydrological cycle and human activities (Doherty et al., 2000; Dentener et al., 2006). Consequently, warmer and wetter atmosphere is likely to intensify the global water cycle that ultimately will result in more frequent and larger flood events.

The space-time distribution of these precipitation regimes is potentially related to the large-scale ocean-atmosphere circulations (Portmann et al., 2009; Yu et al., 2016; Najibi et al., 2017) driven by the natural climatic variability (Trenberth et al., 2007; Zappa et al., 2015). Natural climate variability often causes periods of increasing extremes (flood rich cycle) or decreas-

ing extreme events (flood poor cycle) depending on the phase of the climate (Merz et al., 2014; Hall et al., 2014; Blöschl et al., 2015; Bates, 2016; Armal et al., 2017).

Hence, in an effort to investigate any significant relationship between the observed trend in the flood data (characterized in H1 and H2) and the variability in the climate and atmospheric circulation patterns, we considered large-scale atmospheric teleconnections and climate indices (with quasi-periodicity in nature that can lead to wet-dry regimes) to explain the trend.

4.2.1 Addressing H4: Relationship between observed trend(s) in hypotheses H1 and/or H2 and the atmospheric teleconnections

Our hypothesis (i.e., **H4**) is that the detected time trend is due to cyclical climate influences (i.e., oscillatory behavior) associated with the large-scale ocean-atmospheric interactions as recorded in the ENSO, AMO, PDO, and NAO indices. The corresponding residual time-trend analysis from the models explains whether the long-term natural variability dominates the trends. We considered Poisson distribution as the link function for F_C and $F_{D_{90}}$ and $F_{D_{Median}}$ in the GLM framework since they represent the counts. The detailed information on the GLM's outputs, best choice explanatory variables, and the MK test's outputs on the residuals are shown in Table 8. The most important remarks from Table 8 are given below:

TABLE 8

1. ENSO, AMO, and NAO are related to F_C at the global scale. There is no statistically significant trend in the residuals of the model indicating that the trend initially observed in the global flood frequency data could be attributed to the variability in these indices. AMO and PDO in the tropics, AMO in the subtropics and AMO and PDO in the mid-latitudes (S) are the climate indicators that are dominant in explaining the variability in the flood frequency. The trend in the residuals is non-existent. Together, we can see that the monotonic trend initially observed in the frequency of floods at the global and the sub-spatial scales may be attributed to the variability in the climate and atmospheric teleconnections. Ward et al. (2016) and Emerton et al. (2017) have previously demonstrated the role of ENSO in modulating the global floods. Besides, Hodgkins et al. (2017) demonstrated recently that AMO has a significant negative (positive) relationship with 25 and 50-year flood occurrence for large (medium) catchments in North America (Europe). Our results corroborate with their remarks along with showing that the decadal oscillations also modulates the floods both at the global scale and in each latitudinal belt.

2. We did not find any significant climate indicators that can explain the variability in the median of the floods except for mid-latitude (S). However, as we pointed out before, given the limited data available at this latitudinal belt, we do not further interpret these climate indicators as causing the trends. There should be one or a set of inexplicable factor(s) beyond climate teleconnections that might drive the observed trend in $F_{D_{Median}}$.

3. AMO and NAO have an association with $F_{D_{90}}$ at the global scale. There is no statistically significant trend in the residuals after adjusting for the background variance. In the mid-latitudes (N), the trends in the extreme flood duration values (i.e., $F_{D_{90}}$) can be explained using AMO, PDO, and NAO. In the tropics, AMO, PDO, and NAO are related to the $F_{D_{90}}$, but

we still observe a statistically significant trend after adjusting for this factor. In contrast, the trend in $F_{D_{90}}$ across the subtropics (S) can be related to ENSO, AMO, and NAO. ENSO and NAO can explain the trends across the mid-latitude (S).

In summary:

- **H4**: We have approached the explanation of observed trends in an exploratory spirit and formulated models based on the well-known atmospheric teleconnections. We see that the observed trends in flood frequency across the globe and tropics can be largely linked to the decadal and multi-decadal climate variability. Regarding the flood duration, the observed trends in the median could not be associated with any of these climate factors, while extreme flood duration can be partially associated with AMO for the global and tropics, and ENSO for the southern subtropics and mid-latitudes. We note that the time series (both observed variables and exogenous variables) may have autocorrelation structure that may manifest as trends in limited data. Detection of autocorrelation before ascribing trends is important. We investigated for any structured autocorrelation in the residuals after accounting for the exogenous variables and found none. We did not examine the effect of the lagged dependence of the climate variables here. One can develop models where an appropriate lag can be chosen based on the model performance.

4.3 Comparison of results to recent studies

To our knowledge, this study is the first analysis of "global flood events" that exclusively focuses on the variability of the "flood duration" using the DFO dataset over the last three decades (i.e., 1985-2015). In this part, we are corroborating the presented results here with the most relevant previous studies. However, a high number of recent flood studies have focused on the regional scale, and/or have used the flood duration to calculate the flood magnitude (i.e., Log (duration × severity × affected area)). For instance, Halgamuge and Nirmalathas (2017) analyzed the DFO data from 1985-2016 and concluded that there had been a slight increase in the flood severity in both India and Australia. Similarly, it was reported by Kundzewicz et al. (2014, 2017a, b) that there is an increasing tendency in the number of floods with large magnitude and severity in Europe. These are consistent with our findings.

Several flood-related studies analyzed the trends in the annual maximum streamflow and/or precipitation across multi spatiotemporal scales. For example, an increasing trend in annual maximum precipitation intensities was found by Min et al. (2011) in addition to the increasing trend in the extreme precipitation (Lehmann et al., 2015) at the global scale, but the catchment characteristics and river geomorphology can substantially regulate the streamflow regimes despite the intensified rainfall trends (Hall et al., 2014). Recently, Do et al. (2017) used the Global Runoff Data Center (GRDC) database to investigate the potential trends in the annual maximum streamflow and found the decreasing trends for many stations in western North America but increasing trends in eastern North America, some parts of Europe and South America and southern Africa. A complete comparative analysis is required in this regard, especially to identify the DFO locations with the river basins and then analyze the trends in those river basins. We believe that this involves developing a separate study in the future.

5   Conclusions

A global assessment of flood events is performed here, focusing on the flood frequencies and duration characteristics at different global/latitudinal/country scales from the year 1985 to 2015. The comprehensive assessment of frequencies of flood events and characteristics of probability distribution of flood durations presented here is the very first large-scale study of "actual" flood events worldwide focusing on understanding the temporal changes over the last three decades. It was verified here that the frequency of floods increased at the global scale, tropics, subtropics (S), and mid-latitudes (S). Selected metrics of the flood duration showed a monotonic increasing trend for the median (in all spatial scales), MAD (across the globe, tropics, and subtropics (N)), resistant skewness (across the globe, tropics, subtropics (S) and mid-latitudes (S)), and extremes (all spatial scales except subtropics (N)). More importantly, we find that the frequency of moderate and long duration floods has increased recently, but remain unchanged for the short duration floods in all spatial scales. The trends in the flood frequency and extreme durations at global scale can be largely attributed to ENSO, AMO and NAO, the interannual to decadal to multi-decadal modes of variability. An overall summary is presented below:

- The frequency of flood events has increased; the year 2003 is recognized as the year with the maximum number of flood occurrences across all spatial scales.

- There is a statistically significant trend in the moments of the flood duration at the global scale, tropics, subtropics, and mid-latitudes; the extreme floods post-2000 is more than 30 days as opposed to less than 20 days in the 1980s and 1990s.

- The yearly number of moderate and long duration flood occurrences increased (from before to after the 2000s) by a factor of 4 and 2.5 events per year across the tropics and mid-latitudes (N), respectively.

- There was no monotonic trend observed in the frequencies of short duration floods (i.e. flood duration of 1 to 7 days) across all the spatial scales.

- The increase in frequency of long duration floods during recent years can be related to the persistent patterns in the low-frequency climate indices and atmospheric teleconnections as reported here.

In addition, we also presented a simple overview of the vulnerability profile for different countries. This can be helpful to inform and improve the flood warning systems tailored to the various types and resource management during the post-disaster responses. Furthermore, with increasing globalization, countries are now interdependent through supply chain networks to achieve streamlined production and overall cost reductions. A country level understanding of the exposure to different types of floods can help to predict more accurately, the vulnerable nodes that might cause a systemic network failure. It can also provide the necessary analysis for pricing and portfolio risk management for the agencies that insure and hedge against the flood losses.

While this study explores the trends in the frequency and duration of global floods, especially the long duration floods, it is necessary to investigate the cause-effect mechanism of these trends along with socioeconomic variables to fully understand the

emergence of floods. Understanding these hierarchical layers will provide us with a comprehensive information and realization that can be translated to better define the multi-scale flood risk management and damage control strategies.

Appendix A: Non-parametric trend test

The nonparametric rank-based Mann-Kendall (MK) test is widely applied to detect the monotonic trend (i.e. a gradual change over time with consistency in direction) in climatic or environmental time series (Mann, 1945; Kendall, 1948). It is an appropriate approach to be employed for that type of variables that exhibit skewness around the general relationship (Helsel and Hirsch, 1992). The MK's null hypothesis (H_0) is that there is no monotonic trend (i.e. $-Z_{1-\frac{\alpha}{2}} \leq Z_{MK} \leq Z_{1-\frac{\alpha}{2}}$) (Hirsch, 1992), while a failure to reject H_0 does not confirm the lack of trend in time series. In fact, the provided data are not sufficient to conclude that a trend might be existing, bounded to that specified level of confidence (Meals et al., 2011). The MK test is based on the S statistic as the sum of integers given in the form of the following configuration as:

$$S = \sum_{p=1}^{T-1} \sum_{q=p+1}^{T} \text{Sign}(y_q - y_p); \text{ where } \text{Sign}(y_q - y_p) = \begin{cases} +1 & \text{if } (y_q - y_p) > 0 \\ 0 & \text{if } (y_q - y_p) = 0 \\ -1 & \text{if } (y_q - y_p) < 0 \end{cases} \tag{A1}$$

Also,

$$Z_{MK} = \begin{cases} \frac{S-1}{\sqrt{Var(S)}} & \text{if } S > 0 \\ 0 & \text{if } S = 0 \\ \frac{S+1}{\sqrt{Var(S)}} & \text{if } S < 0 \end{cases} \tag{A2}$$

where T is the total number of observations, y_q and y_p are respectively the data values in the time series p and q ($p{>}q$). Hence, three cases can be associated with the S value derived from Equation A1 (Helsel and Hirsch, 1992) as:

1. It is a large positive number: an upward trend is observed since the later-measured values tend to be larger than earlier ones,

2. It is a large negative number: a downward trend is indicated since the later values tend to be smaller than earlier ones,

3. It is an absolute small number: no trend is indicated.

Further, the Kendall's *Tau* (τ) nonparametric correlation coefficient and Sen's slope (β) (i.e. rate of consistent change) (Sen, 1968) can be computed as:

$$\tau = \frac{S}{\frac{T(T-1)}{2}} \text{ ; and } \beta = median\{\frac{y_q - y_p}{x_q - x_p}\}, p = 1, 2, ..., T-1 \text{ and } q = 2, 3, ..., T \tag{A3}$$

where Kendall's Tau (τ) value is between -1 and +1 (similar to correlation coefficient in linear regression analysis).

Acknowledgements. We are thankful to the Dartmouth Flood Observatory, University of Colorado at Boulder, CO, USA for providing the flood data. This research is supported by:

- Department of Energy Early CAREER (for Naresh Devineni) Award No. DE-SC0018124

- National Science Foundation, Paleo Perspective on Climate Change (P2C2) Program Award No. 1401698

5   • National Science Foundation, Water Sustainability and Climate (WSC) Program Award No. 1360446

We also thank the anonymous reviewers and editor. The statements contained within this research article are not the opinions of the funding agency or the U.S. government but reflect the authors' opinions.

References

Abarbanel, H. D. and Lall, U.: Nonlinear dynamics of the Great Salt Lake: system identification and prediction, Climate Dynamics, 12, 287–297, 1996.

Alexander, L., Zhang, X., Peterson, T., Caesar, J., Gleason, B., Klein Tank, A., Haylock, M., Collins, D., Trewin, B., Rahimzadeh, F., et al.: Global observed changes in daily climate extremes of temperature and precipitation, Journal of Geophysical Research: Atmospheres, 111, 2006.

Armal, S., Devineni, N., and Khanbilvardi, R.: Trends in Extreme Rainfall Frequency in the Contiguous United States: Attribution to Climate Change and Climate Variability Modes, Journal of Climate, 2017.

Barnston, A. G. and Livezey, R. E.: Classification, seasonality and persistence of low-frequency atmospheric circulation patterns, Monthly weather review, 115, 1083–1126, 1987.

Bates, P.: Flooding: what is normal?, Science in Parliament, 73, 25–26, 2016.

Blöschl, G., Gaál, L., Hall, J., Kiss, A., Komma, J., Nester, T., Parajka, J., Perdigão, R. A., Plavcová, L., Rogger, M., et al.: Increasing river floods: fiction or reality?, Wiley Interdisciplinary Reviews: Water, 2, 329–344, 2015.

Bouwer, L. M.: Have disaster losses increased due to anthropogenic climate change?, Bulletin of the American Meteorological Society, 92, 39–46, 2011.

Brakenridge, G., Tracy, B., and Knox, J.: Orbital SAR remote sensing of a river flood wave, International Journal of Remote Sensing, 19, 1439–1445, 1998.

Brakenridge, G., Syvitski, J., Niebuhr, E., Overeem, I., Higgins, S., Kettner, A., and Prades, L.: Design with nature: Causation and avoidance of catastrophic flooding, Myanmar, Earth-Science Reviews, 2016.

Brakenridge, G. R.: Global active archive of large flood events, Dartmouth Flood Observatory, University of Colorado. Available online: http://floodobservatory.colorado.edu/index.html (accessed on 10 September 2014), 2010.

Brakenridge, G. R., Anderson, E., Nghiem, S. V., Caquard, S., and Shabaneh, T. B.: Flood warnings, flood disaster assessments, and flood hazard reduction: The roles of orbital remote sensing, Jet Propulsion Laboratory, National Aeronautics and Space Administration, Pasadena, CA, 2003.

Brakenridge, G. R., Nghiem, S. V., Anderson, E., and Chien, S.: Space-based measurement of river runoff, EOS, Transactions American Geophysical Union, 86, 185–188, 2005.

Brakenridge, G. R., Nghiem, S. V., Anderson, E., and Mic, R.: Orbital microwave measurement of river discharge and ice status, Water Resources Research, 43, 2007.

Brakenridge, G. R., Cohen, S., Kettner, A. J., De Groeve, T., Nghiem, S. V., Syvitski, J. P., and Fekete, B. M.: Calibration of satellite measurements of river discharge using a global hydrology model, Journal of hydrology, 475, 123–136, 2012.

Burkey, J.: A non-parametric monotonic trend test computing Mann-Kendall Tau, Tau-b, and Sen's slope written in Mathworks-MATLAB implemented using matrix rotations, http://www.mathworks.com/matlabcentral/fileexchange/authors/23983, (accessed on 01/25/2016), 2006.

Chandler, R. E. and Wheater, H. S.: Analysis of rainfall variability using generalized linear models: a case study from the west of Ireland, Water Resources Research, 38, 2002.

Dentener, F., Stevenson, D., Ellingsen, K. v., Van Noije, T., Schultz, M., Amann, M., Atherton, C., Bell, N., Bergmann, D., Bey, I., et al.: The global atmospheric environment for the next generation, Environmental Science & Technology, 40, 3586–3594, 2006.

Di Baldassarre, G., Montanari, A., Lins, H., Koutsoyiannis, D., Brandimarte, L., and Blöschl, G.: Flood fatalities in Africa: from diagnosis to mitigation, Geophysical Research Letters, 37, 2010.

Do, H. X., Westra, S., and Leonard, M.: A global-scale investigation of trends in annual maximum streamflow, Journal of Hydrology, 2017.

Doherty, R., Kutzbach, J., Foley, J., and Pollard, D.: Fully coupled climate/dynamical vegetation model simulations over Northern Africa during the mid-Holocene, Climate Dynamics, 16, 561–573, 2000.

ELC: The Environmental Literacy Council, https://enviroliteracy.org/, (accessed on 06/12/2015), 2015.

Emerton, R., Cloke, H., Stephens, E., Zsoter, E., Woolnough, S., and Pappenberger, F.: Complex picture for likelihood of ENSO-driven flood hazard, Nature Communications, 8, 2017.

Enfield, D. B., Mestas-Nuñez, A. M., and Trimble, P. J.: The Atlantic multidecadal oscillation and its relation to rainfall and river flows in the continental US, Geophysical Research Letters, 28, 2077–2080, 2001.

Gabler, R. E., Petersen, J. F., Trapasso, L., and Sack, D.: Physical geography, Nelson Education, 2008.

Gao, L., Zhang, L., and Lu, M.: Characterizing the spatial variations and correlations of large rainstorms for landslide study, Hydrology and Earth System Sciences, 21, 4573, 2017.

Glur, L., Wirth, S. B., Büntgen, U., Gilli, A., Haug, G. H., Schär, C., Beer, J., and Anselmetti, F. S.: Frequent floods in the European Alps coincide with cooler periods of the past 2500 years, Scientific reports, 3, 2770, 2013.

Groisman, P. Y., Knight, R. W., Easterling, D. R., Karl, T. R., Hegerl, G. C., and Razuvaev, V. N.: Trends in intense precipitation in the climate record, Journal of climate, 18, 1326–1350, 2005.

Guha-Sapir, D., Below, R., and Hoyois, P.: EM-DAT: The CRED, OFDA International Disaster Database–www. emdat. be–Université Catholique de Louvain–Brussels–Belgium, 2016.

Halgamuge, M. N. and Nirmalathas, T.: Analysis of Large Flood Events: Based on Flood Data During 1985–2016 in Australia and India, International Journal of Disaster Risk Reduction, 2017.

Hall, J., Arheimer, B., Borga, M., Brázdil, R., Claps, P., Kiss, A., Kjeldsen, T., Kriauciuniene, J., Kundzewicz, Z., Lang, M., et al.: Understanding flood regime changes in Europe: A state of the art assessment, Hydrology and earth system sciences, 18, 2735–2772, 2014.

Hallegatte, S., Green, C., Nicholls, R. J., and Corfee-Morlot, J.: Future flood losses in major coastal cities, Nature Climate Change, 3, 802–806, 2013.

Hampel, F. R.: The influence curve and its role in robust estimation, Journal of the American Statistical Association, 69, 383–393, 1974.

Haraguchi, M. and Lall, U.: Flood risks and impacts: A case study of Thailand's floods in 2011 and research questions for supply chain decision making, International Journal of Disaster Risk Reduction, 14, 256–272, 2015.

Hashimoto, T., Stedinger, J. R., and Loucks, D. P.: Reliability, resiliency, and vulnerability criteria for water resource system performance evaluation, Water resources research, 18, 14–20, 1982.

Helsel, D. R. and Hirsch, R. M.: Statistical methods in water resources, vol. 49, Elsevier, 1992.

Hirabayashi, Y., Mahendran, R., Koirala, S., Konoshima, L., Yamazaki, D., Watanabe, S., Kim, H., and Kanae, S.: Global flood risk under climate change, Nature Climate Change, 3, 816–821, 2013.

Hirsch, R.: Statistical Methods in Water Resources. Studies in Environmental Science, Elsevier Science & Technology, 1992.

Hodgkins, G. A., Whitfield, P. H., Burn, D. H., Hannaford, J., Renard, B., Stahl, K., Fleig, A. K., Madsen, H., Mediero, L., Korhonen, J., et al.: Climate-driven variability in the occurrence of major floods across North America and Europe, Journal of Hydrology, 552, 704–717, 2017.

Holling, C. S.: Myth of Ecological Stability: Resilience and the Problem of Failure, Studies on crisis management, 4, 1978.

Hurrell, J. W. and Van Loon, H.: Decadal variations in climate associated with the North Atlantic Oscillation, in: Climatic Change at High Elevation Sites, pp. 69–94, Springer, 1997.

Jongman, B., Ward, P. J., and Aerts, J. C.: Global exposure to river and coastal flooding: Long term trends and changes, Global Environmental Change, 22, 823–835, 2012.

5 Karamperidou, C., Cane, M. A., Lall, U., and Wittenberg, A. T.: Intrinsic modulation of ENSO predictability viewed through a local Lyapunov lens, Climate dynamics, 42, 253–270, 2014.

Kendall, M. G.: Rank correlation methods., 1948.

Kundzewicz, Z., Krysanova, V., Dankers, R., Hirabayashi, Y., Kanae, S., Hattermann, F., Huang, S., Milly, P., Stoffel, M., Driessen, P., et al.: Differences in flood hazard projections in Europe–their causes and consequences for decision making, Hydrological Sciences Journal, 62,

10 1–14, 2017a.

Kundzewicz, Z. W., Kanae, S., Seneviratne, S. I., Handmer, J., Nicholls, N., Peduzzi, P., Mechler, R., Bouwer, L. M., Arnell, N., Mach, K., et al.: Flood risk and climate change: global and regional perspectives, Hydrological Sciences Journal, 59, 1–28, 2014.

Kundzewicz, Z. W., Pińskwar, I., and Brakenridge, G. R.: Changes in river flood hazard in Europe: a review, Hydrology Research, p. nh2017016, 2017b.

15 Lehmann, J., Coumou, D., and Frieler, K.: Increased record-breaking precipitation events under global warming, Climatic Change, 132, 501–515, 2015.

Leys, C., Ley, C., Klein, O., Bernard, P., and Licata, L.: Detecting outliers: Do not use standard deviation around the mean, use absolute deviation around the median, Journal of Experimental Social Psychology, 49, 764–766, 2013.

Liu, C. and Zipser, E. J.: The global distribution of largest, deepest, and most intense precipitation systems, Geophysical Research Letters,

20 42, 3591–3595, 2015.

Liu, X., Liu, Z., Zhang, Y., and Jiang, B.: The Effects of Floods on the Incidence of Bacillary Dysentery in Baise (Guangxi Province, China) from 2004 to 2012, International Journal of Environmental Research and Public Health, 14, 179, 2017.

Lowe, D., Ebi, K. L., and Forsberg, B.: Factors increasing vulnerability to health effects before, during and after floods, International journal of environmental research and public health, 10, 7015–7067, 2013.

25 Lu, M. and Hao, X.: Diagnosis of the Tropical Moisture Exports to the Mid-Latitudes and the Role of Atmospheric Steering in the Extreme Precipitation, Atmosphere, 8, 2017.

Lu, M. and Lall, U.: Tropical Moisture Exports, Extreme Precipitation and Floods in Northeastern US, Earth Science Research, 6, 91, 2017.

Lu, M., Lall, U., Schwartz, A., and Kwon, H.: Precipitation predictability associated with tropical moisture exports and circulation patterns for a major flood in France in 1995, Water Resources Research, 49, 6381–6392, 2013.

30 Mann, H. B.: Nonparametric tests against trend, Econometrica: Journal of the Econometric Society, pp. 245–259, 1945.

McCullagh, P.: Generalized linear models, European Journal of Operational Research, 16, 285–292, 1984.

Meals, D., Spooner, J., Dressing, S., and Harcum, J.: Statistical analysis for monotonic trends, Tech Notes, 6, 23, 2011.

Merz, B., Aerts, J., Arnbjerg-Nielsen, K., Baldi, M., Becker, A., Bichet, A., Blöschl, G., Bouwer, L., Brauer, A., Cioffi, F., et al.: Floods and climate: emerging perspectives for flood risk assessment and management, Natural Hazards and Earth System Sciences, 14, 1921, 2014.

35 Milojevic, A., Armstrong, B., Kovats, S., Butler, B., Hayes, E., Leonardi, G., Murray, V., and Wilkinson, P.: Long-term effects of flooding on mortality in England and Wales, 1994-2005: controlled interrupted time-series analysis, Environmental Health, 10, 11, 2011.

Min, S.-K., Zhang, X., Zwiers, F. W., and Hegerl, G. C.: Human contribution to more-intense precipitation extremes, Nature, 470, 378–381, 2011.

Mirza, M. M. Q.: Climate change and extreme weather events: can developing countries adapt?, Climate policy, 3, 233–248, 2003.

Najibi, N., Devineni, N., and Lu, M.: Hydroclimate drivers and atmospheric teleconnections of long duration floods: An application to large reservoirs in the Missouri River Basin, Advances in Water Resources, 100, 153–167, 2017.

Nakamura, J., Lall, U., Kushnir, Y., Robertson, A. W., and Seager, R.: Dynamical structure of extreme floods in the US Midwest and the United Kingdom, Journal of Hydrometeorology, 14, 485–504, 2013.

Peduzzi, P., Dao, H., Herold, C., and Mouton, F.: Assessing global exposure and vulnerability towards natural hazards: the Disaster Risk Index, Natural Hazards and Earth System Sciences, 9, 1149–1159, 2009.

Peduzzi, P., Herold, C., Mouton, F., Dao, H., Gregory, G., and Chatenoux, B.: Global human exposure to flood hazard, http://preview.grid.unep.ch, (accessed on 01/25/2016), 2011.

Perdigão, R. and Blöschl, G.: Dynamics of the flood response to slow-fast landscape-climate feedbacks, Proceedings of the International Association of Hydrological Sciences, 370, 125–130, 2015.

Portmann, R. W., Solomon, S., and Hegerl, G. C.: Spatial and seasonal patterns in climate change, temperatures, and precipitation across the United States, Proceedings of the National Academy of Sciences, 106, 7324–7329, 2009.

Promchote, P., Simon Wang, S.-Y., and Johnson, P. G.: The 2011 great flood in Thailand: Climate diagnostics and Implications from climate change, Journal of Climate, 29, 367–379, 2016.

Rayner, N., Parker, D. E., Horton, E., Folland, C., Alexander, L., Rowell, D., Kent, E., and Kaplan, A.: Global analyses of sea surface temperature, sea ice, and night marine air temperature since the late nineteenth century, Journal of Geophysical Research: Atmospheres, 108, 2003.

Robertson, A. W., Kushnir, Y., Lall, U., and Nakamura, J.: On the connection between low-frequency modulation of large-scale weather regimes and springtime extreme flooding over the midwest of the United States, Science and Technology Infusion Climate Bulletin. Fort Worth, TX, USA, pp. 150–152, 2011.

Sachs, L.: Applied statistics: a handbook of techniques, Springer Science & Business Media, 2012.

Schiermeier, Q.: Increased flood risk linked to global warming: likelihood of extreme rainfall may have been doubled by rising greenhouse-gas levels, Nature, 470, 316–317, 2011.

Schultz, B.: Flood management under rapid urbanisation and industrialisation in flood-prone areas: a need for serious consideration, Irrigation and drainage, 55, 2006.

Sen, P. K.: Estimates of the regression coefficient based on Kendall's tau, Journal of the American Statistical Association, 63, 1379–1389, 1968.

Singh, A. and Zommers, Z., eds.: Reducing Disaster: Early Warning Systems For Climate Change, Springer Netherlands, 2014.

Solomon, S.: Climate change 2007-the physical science basis: Working group I contribution to the fourth assessment report of the IPCC, vol. 4, Cambridge University Press, 2007.

Stevens, A. J., Clarke, D., and Nicholls, R. J.: Trends in reported flooding in the UK: 1884–2013, Hydrological Sciences Journal, 61, 50–63, 2016.

Thenkabail, P. S.: Remotely Sensed Data Characterization, Classification, and Accuracies, CRC Press, 2015.

Thomalla, F., Downing, T., Spanger-Siegfried, E., Han, G., and Rockström, J.: Reducing hazard vulnerability: towards a common approach between disaster risk reduction and climate adaptation, Disasters, 30, 39–48, 2006.

Trenberth, K. E.: Atmospheric moisture recycling: Role of advection and local evaporation, Journal of Climate, 12, 1368–1381, 1999.

Trenberth, K. E.: Changes in precipitation with climate change, Climate Research, 47, 123–138, 2011.

Trenberth, K. E., Dai, A., Rasmussen, R. M., and Parsons, D. B.: The changing character of precipitation, Bulletin of the American Meteorological Society, 84, 1205–1217, 2003.

Trenberth, K. E., Smith, L., Qian, T., Dai, A., and Fasullo, J.: Estimates of the global water budget and its annual cycle using observational and model data, Journal of Hydrometeorology, 8, 758–769, 2007.

5   Van Dijk, A. I., Brakenridge, G. R., Kettner, A. J., Beck, H. E., De Groeve, T., and Schellekens, J.: River gauging at global scale using optical and passive microwave remote sensing, Water Resources Research, 52, 6404–6418, 2016.

Vogel, R. M., Yaindl, C., and Walter, M.: Nonstationarity: Flood magnification and recurrence reduction factors in the United States, JAWRA Journal of the American Water Resources Association, 47, 464–474, 2011.

Walker, C. C. and Schneider, T.: Response of idealized Hadley circulations to seasonally varying heating, Geophysical research letters, 32,
10   2005.

Ward, P., Kummu, M., and Lall, U.: Flood frequencies and durations and their response to El Niño Southern Oscillation: Global analysis, Journal of Hydrology, 539, 358–378, 2016.

Ward, P. J., Jongman, B., Salamon, P., Simpson, A., Bates, P., De Groeve, T., Muis, S., De Perez, E. C., Rudari, R., Trigg, M. A., et al.: Usefulness and limitations of global flood risk models, Nature Climate Change, 5, 712–715, 2015.

15   Westra, S., Alexander, L. V., and Zwiers, F. W.: Global increasing trends in annual maximum daily precipitation, Journal of Climate, 26, 3904–3918, 2013.

Yang, C., Chandler, R., Isham, V., and Wheater, H.: Spatial-temporal rainfall simulation using generalized linear models, Water Resources Research, 41, 2005.

Yu, L., Zhong, S., Pei, L., Bian, X., and Heilman, W. E.: Contribution of large-scale circulation anomalies to changes in extreme precipitation
20   frequency in the United States, Environmental Research Letters, 11, 044 003, 2016.

Zappa, G., Hawcroft, M. K., Shaffrey, L., Black, E., and Brayshaw, D. J.: Extratropical cyclones and the projected decline of winter Mediterranean precipitation in the CMIP5 models, Climate Dynamics, 45, 1727–1738, 2015.

Zhai, J. and Boos, W.: Regime transitions of cross-equatorial Hadley circulations with zonally asymmetric thermal forcings, Journal of the Atmospheric Sciences, 72, 3800–3818, 2015.

25   Zhang, Y., Wallace, J. M., and Battisti, D. S.: ENSO-like interdecadal variability: 1900–93, Journal of climate, 10, 1004–1020, 1997.

Zhou, Y., Lau, W. K., and Liu, C.: Rain characteristics and large-scale environments of precipitation objects with extreme rain volumes from TRMM observations, Journal of Geophysical Research: Atmospheres, 118, 9673–9689, 2013.

Ziegler, A. D., Lim, H. S., Tantasarin, C., Jachowski, N. R., and Wasson, R.: Floods, false hope, and the future, Hydrological Processes, 26, 1748–1750, 2012.

Figure 1. Spatial segmentation to assign the global flood events (1985 to 2015) into different latitudinal belts; Mid-latitudes (N): 55 ºN-35 ºN, Subtropics (N): 35 ºN-23.5 ºN, Tropics (N): 23.5 ºS-23.5 ºN, Subtropics (S): 35 ºS-23.5 ºS, and Mid-latitudes (S): 55 ºS-35 ºS; (N) and (S) indicate Northern and Southern hemisphere, respectively; the four rounded rectangles shows the United States of America (USA), China, India and Thailand.
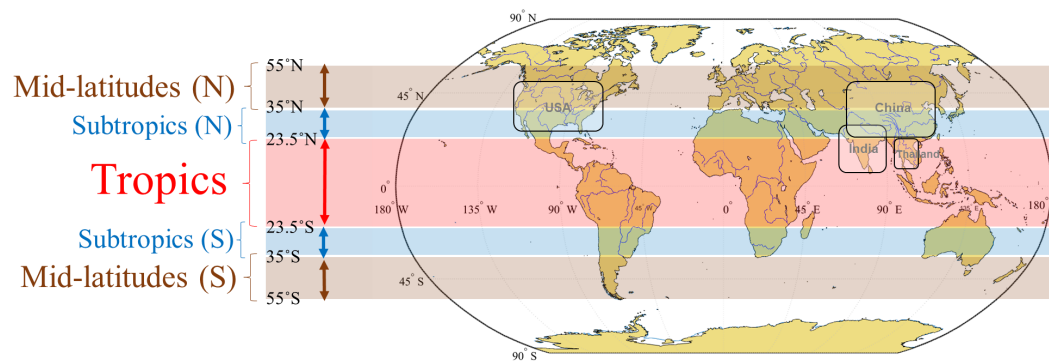
Figure 2. Frequency of flood events at the global scale and the latitudinal scales (i.e. Tropics, Subtropics (N), Subtropics (S), Mid-latitudes (N), and Mid-latitudes (S)); a solid line LOESS curve fitting is shown for the time-series where a significant trend on number of flood events is observed (Mann-Kendall Test with significance level $\alpha = 0.05$), while the dashed line indicates the LOESS curve for the regions with insignificant trend.
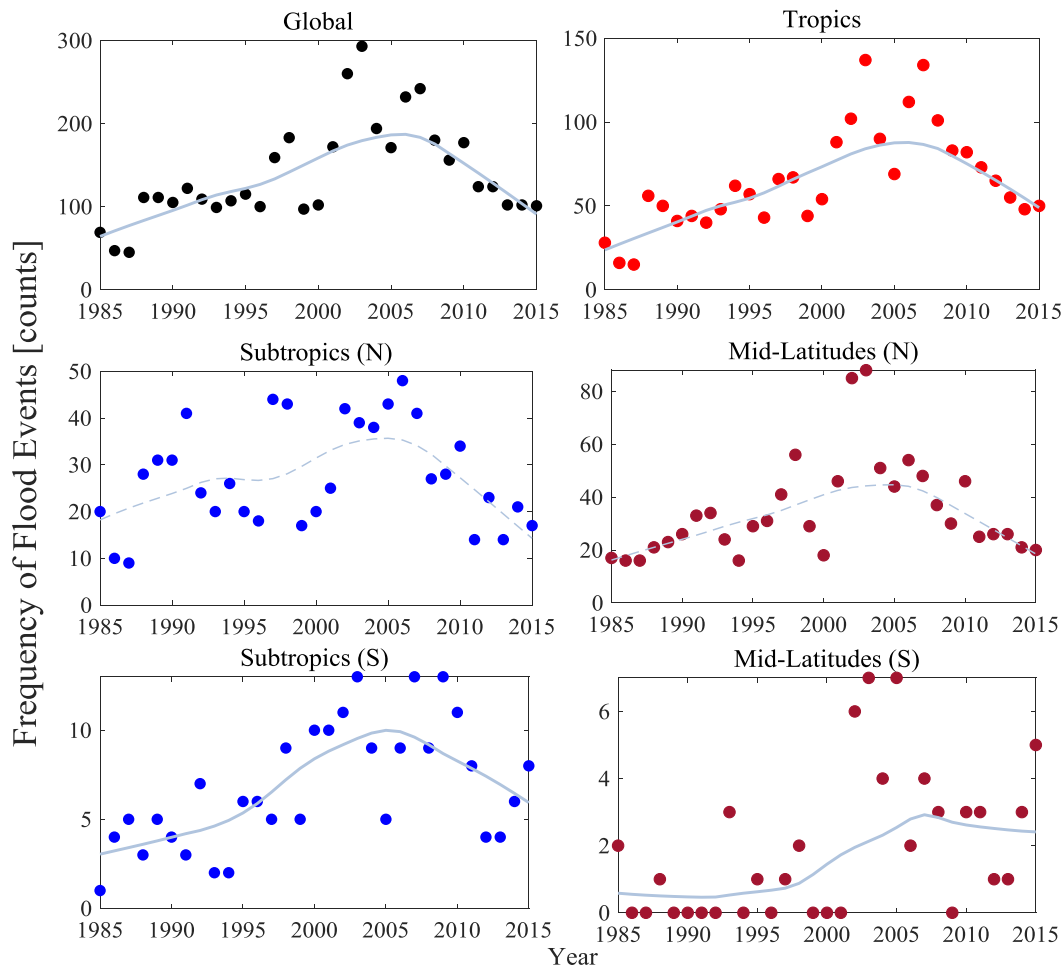
Figure 3. Same as Figure 2 but for Median of flood durations.
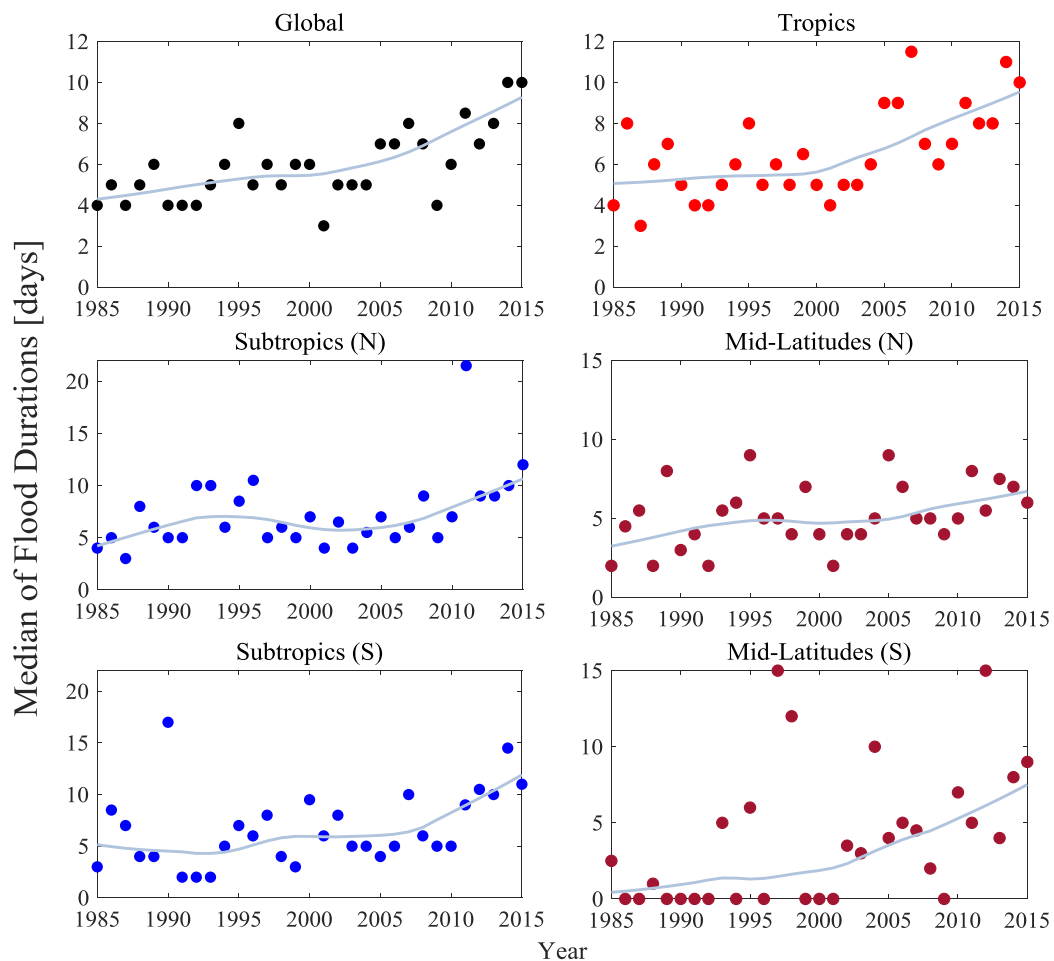
Figure 4. Same as Figure 2 but for Median Absolute Deviation (MAD) of flood durations.
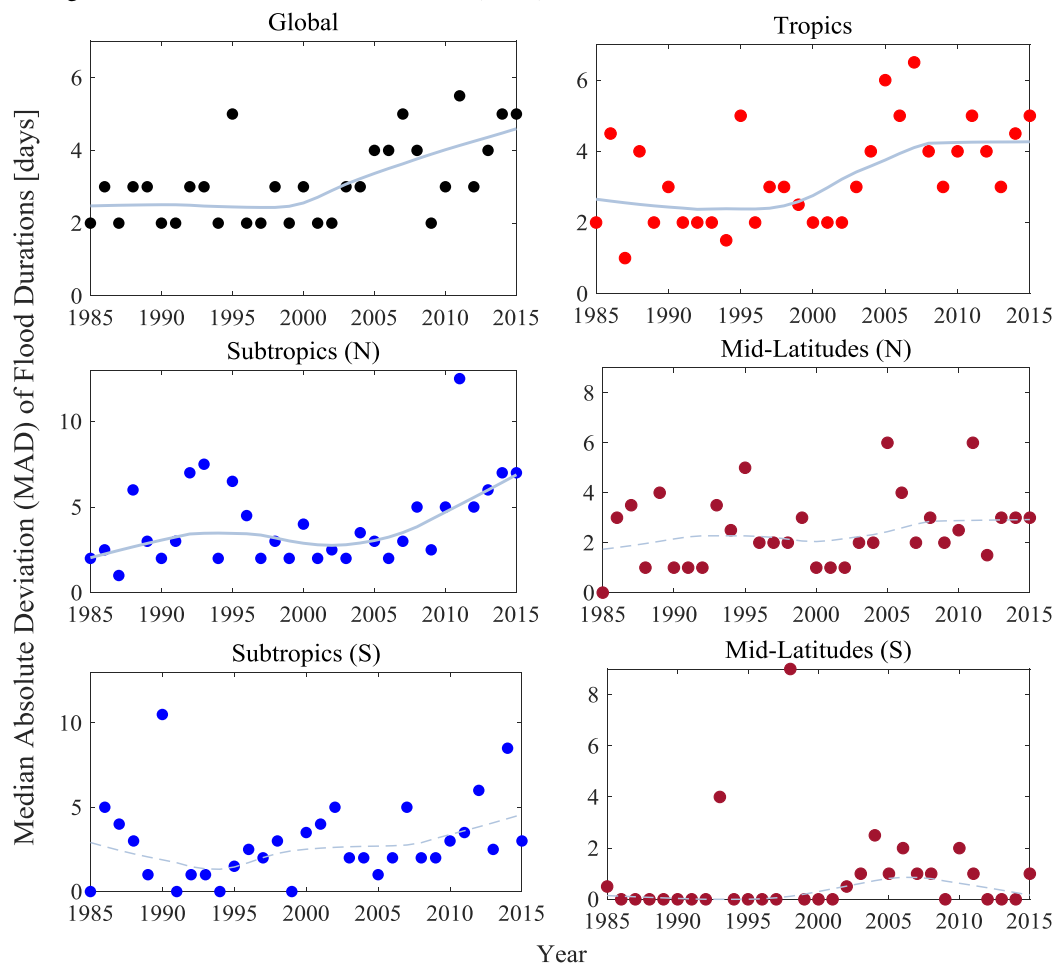
Figure 5. Same as Figure 2 but for the resistant Skewness of flood durations.
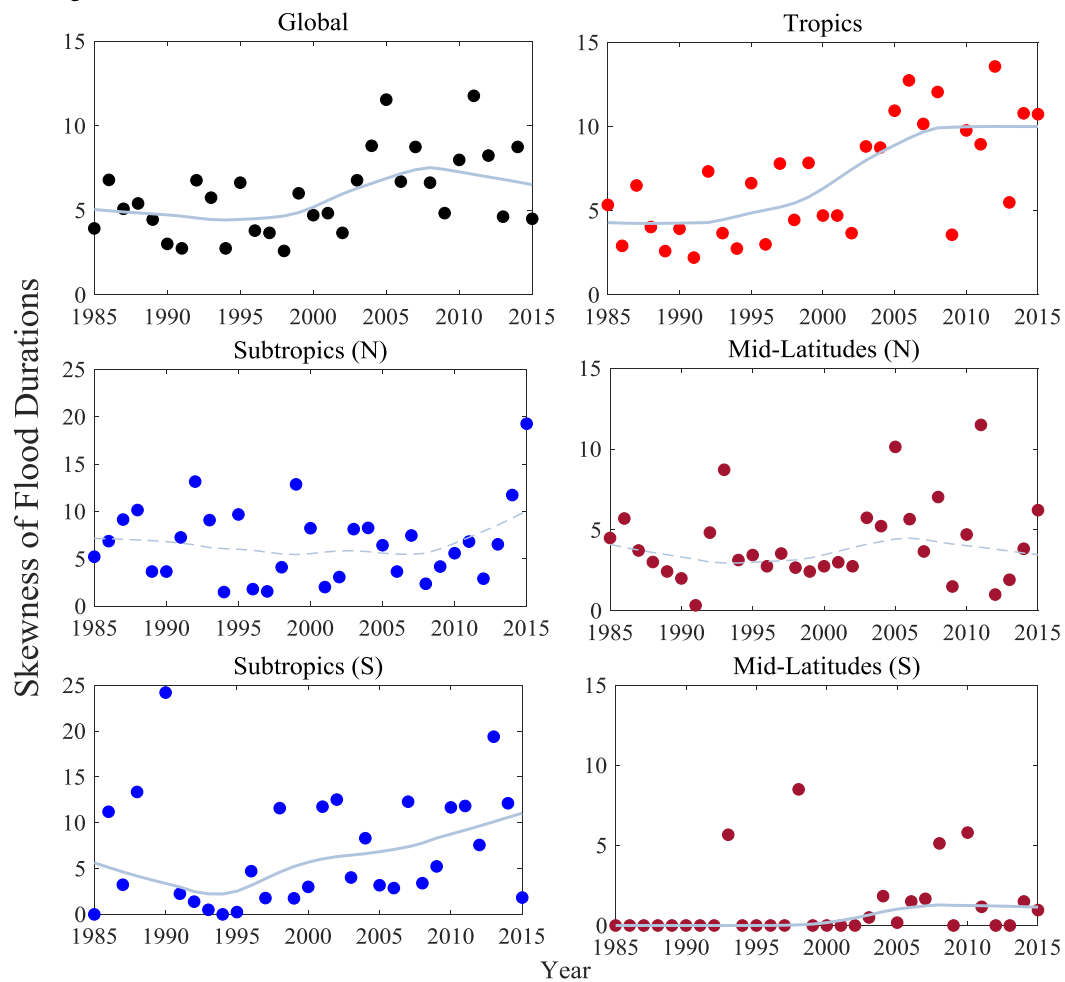
Figure 6. Same as Figure 2 but for the 90th percentile of flood durations.
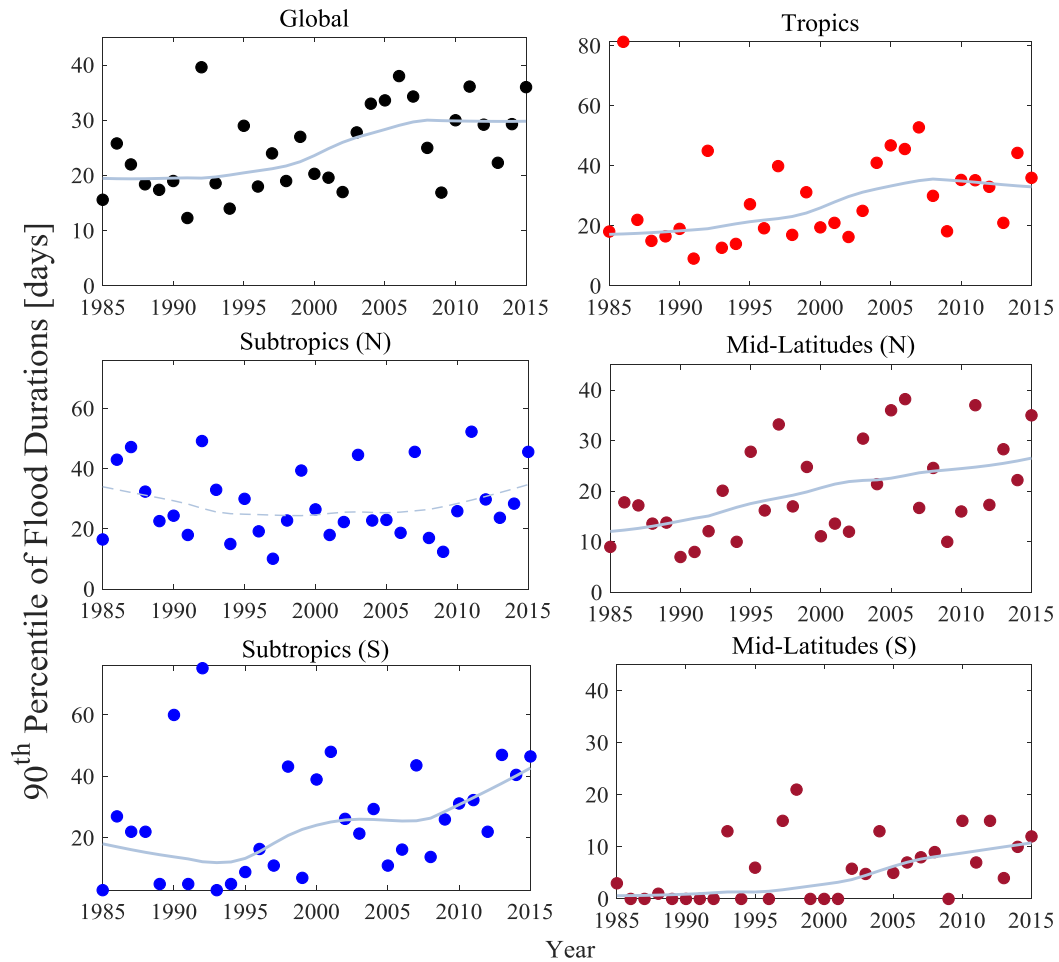
Figure 7. **(a)** Relative frequency of short (less than 7 days), moderate (8 to 21 days) and long duration (21 days and above) floods for the countries with at least 31 events from 1985 to 2015; **(b)** Relative flood damages due to short, moderate and long duration floods with respect to total flood damages for the countries with at least 31 events from 1985 to 2015 (except Colombia, Peru, Ethiopia, Somalia, and Afghanistan due to lack of data)
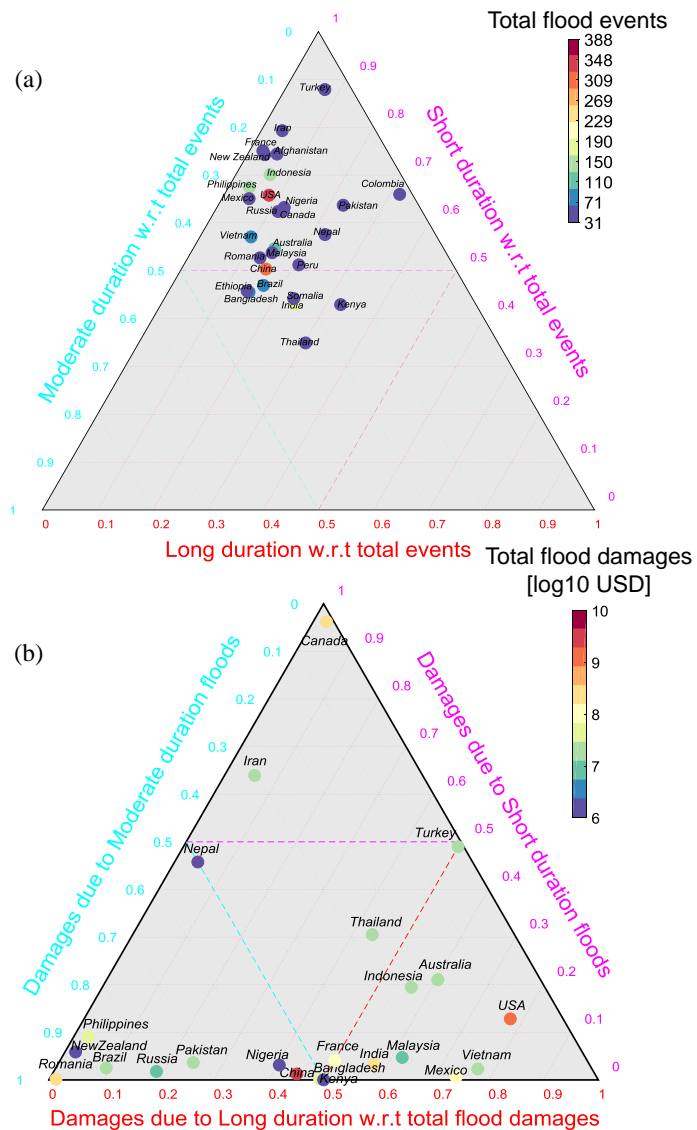
Figure 8. (a) Covariation of flood duration with the corresponding flood damages for top four countries with the maximum number of long duration flood events (i.e., India, China, USA, and Thailand),**(b)** Total number of short (less than 7 days), moderate (8 to 21 days) and long duration (21 days and above) floods, and **(c)** Total damages due to short, moderate and long duration floods. These countries are the top 21 countries which are ranked based on the frequency of each flood duration category and corresponding flood damages using the DFO flood data from 1985 to 2015.
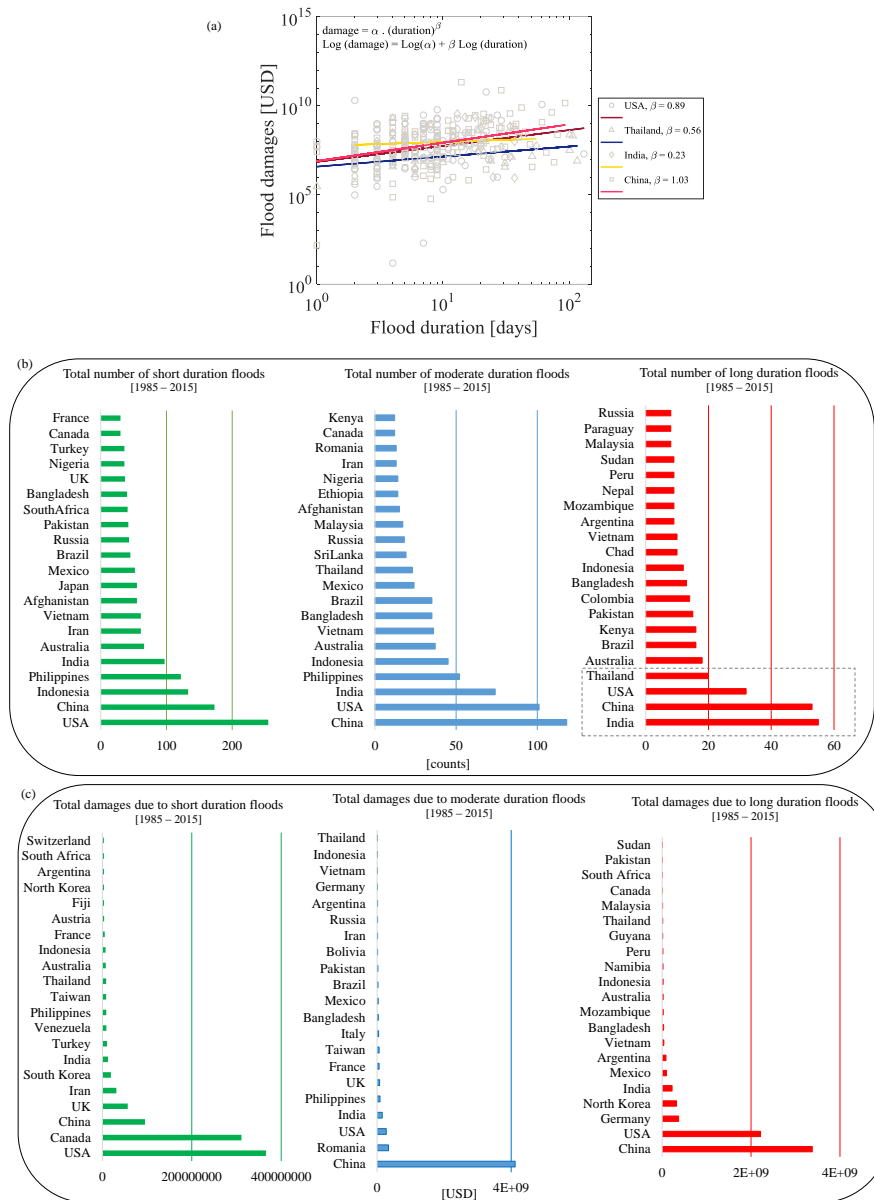
Table 1. Proposed hypotheses and evaluation approach.

Hypothesis	Evaluation Strategy
H1 There is no monotonic trend in the annual frequency of flood events globally and in different latitudinal belts.	▶Non-parametric Mann-Kendall trend test is applied on the annual time series of flood counts ($F_C{}^{t,r}$).
H2 There is no monotonic trend in the distribution of flood duration globally and in different latitudinal belts.	▶Non-parametric Mann-Kendall trend test is applied on the annual time series of median, median absolute deviation, resistant skewness, and 90th percentile of flood duration's distributions ($\boldsymbol{F_D}{}^{t,r}$).
H3 There is no monotonic trend in the annual frequency of short, moderate and long duration flood events in different latitudinal belts.	▶Non-parametric Mann-Kendall trend test is applied on the annual time series of short, moderate and long duration flood events ($F_{CS}{}^{t,r}$, $F_{CM}{}^{t,r}$, $F_{CL}{}^{t,r}$).
H4 Any observed trend(s) in **H1** and/or **H2** is related to the atmospheric teleconnections.	▶Generalized Linear Models are developed for $F_C{}^{t,r}$ and $\boldsymbol{F_D}{}^{t,r}$ using the climate indices; Mann-Kendall trend test is applied on the residual of models.

Table 2. Summary of Trend analysis (Mann-Kendall Test with significance level $\alpha = 0.05$) on the frequencies (occurrences) of flood events at the global scale and five latitudinal belts.

Spatial Scale	Frequency of Flood Events (1985 − 2015)					
	Trend Analysis					
	Total flood events	Maximum number of floods occurred in any given year	Kendall's Tau	Sen's slope	*p*-value (two tailed test)	Trend
Global	4311	293	0.26	2.12	0.0429	✓
Mid-Latitudes (North)	1077	88	0.22	0.5	0.086	✗
Subtropics (North)	856	48	0.032	0.048	0.8115	✗
Tropics	2020	137	0.4	1.74	0.0016	✓
Subtropics (South)	210	13	0.366	0.22	0.0038	✓
Mid-Latitudes (South)	59	7	0.327	0.083	0.0077	✓

Table 3. Summary of Trend analysis (Mann-Kendall Test with significance level $\alpha = 0.05$) on the median of flood durations at the global scale and five latitudinal belts.

Spatial Scale	Median of Flood Durations (1985 − 2015)					
	Trend Analysis					
	Median of flood durations [days]	Maximum flood durations in any given year	Kendall's Tau	Sen's slope	p-value (two tailed test)	Trend
Global	6	168	0.484	0.125	0.000103	✓
Mid-Latitudes (North)	5	131	0.2667	0.0909	0.0346	✓
Subtropics (North)	6	122	0.3097	0.125	0.0141	✓
Tropics	6	168	0.4473	0.15	0.00037	✓
Subtropics (South)	6	93	0.3312	0.1667	0.0088	✓
Mid-Latitudes (South)	5	21	0.3613	0.2105	0.0034	✓

Table 4. Summary of Trend analysis (Mann-Kendall Test with significance level $\alpha = 0.05$) on the median absolute deviation (MAD) of flood durations at the global scale and five latitudinal belts.

Spatial Scale	Median Absolute Deviation (MAD) of Flood Durations $(1985 - 2015)$					
	Trend Analysis					
	Median of MAD of entire flood durations	Maximum flood durations in any given year	Kendall's Tau	Sen's slope	p-value (two tailed test)	Trend
Global	3	5.5	0.372	0.0588	0.0021	✓
Mid-Latitudes (North)	2	6	0.1892	0.0417	0.1323	✗
Subtropics (North)	3	12.5	0.2817	0.0909	0.0251	✓
Tropics	3	6.5	0.3763	0.0833	0.0025	✓
Subtropics (South)	2.5	10.5	0.2409	0.0769	0.0570	✗
Mid-Latitudes (South)	0	9	0.1914	0.00001	0.0924	✗

Table 5. Summary of Trend analysis (Mann-Kendall Test with significance level $\alpha = 0.05$) on resistant skewness of flood duration distributions at the global scale and five latitudinal belts.

Spatial Scale	Resistant Skewness of Flood Duration Distributions $(1985 - 2015)$					
	Trend Analysis					
	Median of skewness of flood distributions	Average of skewness of flood distributions	Kendall's Tau	Sen's slope	p-value (two tailed test)	Trend
Global	5.41	5.89	0.2731	0.1146	0.0321	✔
Mid-Latitudes (North)	3.5395	4.1903	0.0925	0.0386	0.4750	✕
Subtropics (North)	6.5385	6.6653	0.0129	0.0084	0.9322	✕
Tropics	6.5	6.7885	0.4839	0.2468	0.00014	✔
Subtropics (South)	4.0227	6.6652	0.2839	0.2017	0.0260	✔
Mid-Latitudes (South)	0	1.1096	0.2903	0	0.0092	✔

Table 6. Summary of Trend analysis (Mann-Kendall Test with significance level $\alpha = 0.05$) on 90th percentile of flood duration distributions at the global scale and five latitudinal belts.

Spatial Scale	90th Percentile of Flood Durations (1985 − 2015)					
	Trend Analysis					
	Median of 90th percentile flood duration per year [days]	Maximum of 90th percentile flood duration in any given year	Kendall's Tau	Sen's slope	*p*-value (two tailed test)	Trend
Global	24	39.6	0.3699	0.4417	0.0037	✓
Mid-Latitudes (North)	17.2	38.2	0.3355	0.4875	0.0084	✓
Subtropics (North)	24.4	52.3	0.0452	0.0750	0.7338	✗
Tropics	25	81.3	0.3054	0.6364	0.0165	✓
Subtropics (South)	22	75.2	0.2946	0.7385	0.0206	✓
Mid-Latitudes (South)	4.8	21	0.3570	0.3182	0.0038	✓

Table 7. Summary of Trend analysis (Mann-Kendall Test with significance level $\alpha = 0.05$) on three flood classes; short, moderate and long durations of flood events over five latitudinal belts.

Climate Zone	Total flood events [1985 to 2015]	Maximum number of floods in any given year	Test Result	Standard deviation	Kendall's Tau	Sen's slope	*p*-value (two tailed test)	Trend
Short Duration (1 to 7 days)								
Mid-Latitudes (North)	724	68	Cannot Reject	-	-	-	-	✗
Subtropics (North)	496	34	Cannot Reject	-	-	-	-	✗
Tropics	1125	88	Cannot Reject	-	-	-	-	✗
Subtropics (South)	121	8	Cannot Reject	-	-	-	-	✗
Mid-Latitudes (South)	42	7	Cannot Reject	-	-	-	-	✗
Moderate Duration (8 to 20 days)								
Mid-Latitudes (North)	256	20	Cannot Reject	-	-	-	-	✗
Subtropics (North)	235	15	Cannot Reject	-	-	-	-	✗
Tropics	586	48	Reject	58.6231	0.4602	0.6667	0.00028	✓
Subtropics (South)	58	5	Reject	57.4	0.4022	0.0909	0.0012	✓
Mid-Latitudes (South)	16	4	Cannot Reject	-	-	-	-	✗
Long Duration (21 days and above)								
Mid-Latitudes (North)	97	11	Reject	58.0345	0.357	0.1111	0.0045	✓
Subtropics (North)	125	8	Cannot Reject	-	-	-	-	✗
Tropics	306	37	Reject	58.6174	0.5462	0.5417	0.0000158	✓
Subtropics (South)	31	4	Cannot Reject	-	-	-	-	✗
Mid-Latitudes (South)	1	1	Cannot Reject	-	-	-	-	✗

Table 8. Summary of Generalized Linear Model (GLM) results relating selected predictors to flood frequency (F_C), median and 90th percentile of flood durations (F_D) for the global scale and over five latitudinal belts from 1985 to 2015.

Trend (✓ or –)	Model	Descriptive Formula		Global	Mid-Latitudes (North)	Subtropics (North)	Tropics	Subtropics (South)	Mid-Latitudes (South)
F_C	GLM (Poisson)	*Trend in flood data*		✓	–	–	✓	✓	✓
		$a+b_1ENSO+b_2AMO+b_3PDO+b_4NAO$		a,b_1,b_2,b_3	–	–	a,b_2,b_3	a,b_2	a,b_2,b_3
		MK Test on Residuals	*p-value =*	0.81	–	–	0.54	0.18	0.27
		Potential Driver		ENSO, AMO, NAO	–	–	AMO, PDO	AMO	AMO, PDO
$F_{D_{Median}}$	GLM (Log-Normal)	*Trend in flood data*		✓	✓	✓	✓	✓	✓
		$a+b_1ENSO+b_2AMO+b_3PDO+b_4NAO$		a	a	a	a	a	a,b_1,b_4
		MK Test on Residuals	*p-value =*	0.0001	0.03	0.06	0.0003	0.008	0.23
		Potential Driver		Unexplained Factor(s)	Unexplained Factor(s)	No Factor	Unexplained Factor(s)	Unexplained Factor(s)	ENSO, NAO
$F_{D_{90}}$	GLM (Poisson)	*Trend in flood data*		✓	✓	–	✓	✓	✓
		$a+b_1ENSO+b_2AMO+b_3PDO+b_4NAO$		a,b_2,b_4	a,b_2,b_3,b_4	–	a,b_2,b_3,b_4	a,b_1,b_2,b_4	a,b_1,b_4
		MK Test on Residuals	*p-value =*	0.13	0.3	–	0.04	0.17	0.2
		Potential Driver		AMO, NAO	AMO, PDO, NAO	–	AMO, PDO, NAO, Unexplained Factor(s)	ENSO, AMO, NAO	ENSO, NAO